

Large-Area UAS-Based Forest Health Monitoring Utilizing a Hydrogen-Powered Airship and Multispectral Imaging

Emma Turkulainen¹, Janne Hietala², Jiri Jormakka², Johanna Tuviala³, Raquel Alves de Oliveira¹, Niko Koivumäki¹, Kirsi Karila¹, Roope Näsi¹, Juha Suomalainen¹, Mikko Pelto-Arvo³, Päivi Lyytikäinen-Saarenmaa¹, Eija Honkavaara¹

¹ Department of Remote Sensing and Photogrammetry, Finnish Geospatial Research Institute in National Land Survey of Finland (FGI), 02150 Espoo, Finland – emma.turkulainen@nls.fi, raquel.alvesdeoliveira@nls.fi, niko.koivumaki@nls.fi, kirsi.karila@nls.fi, roope.nasi@nls.fi, juha.suomalainen@nls.fi, paivi.lyytikainen-saarenmaa@nls.fi, eija.honkavaara@nls.fi

² Kelluu Ltd. Metallimiehentie 4, 80330 Reijola, Finland – janne@kelluu.com, jiri@kelluu.com

³ School of Forest Sciences, University of Eastern Finland, 80100 Joensuu, Finland – johanna.tuviala@uef.fi, mikko.pelto-arvo@uef.fi, paivi.lyytikainen-saarenmaa@uef.fi

Keywords: Bark beetle, BVLOS, Classification, Deep learning, Multispectral, UAS

Abstract

Climate change is threatening forest ecosystems worldwide by inducing various abiotic and biotic disturbances. In Europe, the European spruce bark beetle (*Ips typographus* L.) poses a significant threat, causing serious mortality in mature Norway spruce (*Picea abies* H. Karst.) stands. Rapidly evolving remote sensing technologies offer valuable tools for monitoring forest health, enabling timely management operations. This study presents a novel approach for large-area forest health monitoring using Uncrewed Aircraft Systems (UAS) and multispectral imaging. The research focuses on a hydrogen-powered Beyond Visual Line of Sight (BVLOS) airship for efficient monitoring of disturbances caused by *I. typographus*. A specific challenge is training machine learning models capable of covering wide areas. Our objective was to study the potential of deep learning models, including transfer learning and fine-tuning techniques, in developing the scalability and accuracy of UAS-based monitoring for detecting individual spruce trees and classifying their health. The approach was empirically evaluated in a study site in North Karelia, Finland. A multispectral image dataset was collected over a 1.3 km² test area in May 2023 in a BVLOS setting operated from a command centre 75 km away. The results indicated that employing transfer learning significantly improved classification accuracy compared to training models from scratch, showing potential for implementing scalable machine learning methods for large-area UAS surveys. The best model yielded F1-scores of 0.936 for healthy, 0.955 for dead, and 0.817 for non-spruce classes. Furthermore, the results indicated that BVLOS airships offered high accuracy while reducing emissions and labour associated with UAS monitoring.

1. Introduction

Climate change is causing various abiotic and biotic disturbances that threaten forest ecosystems worldwide. In Europe, the European spruce bark beetle (*Ips typographus* L.) is notably impacting Norway spruce (*Picea abies* H. Karst.) forests, resulting in significant tree mortality (Patacca et al., 2023; Barrere et al., 2023). Effective monitoring strategies and forest health assessment methods are essential to mitigate the economic and ecological damages caused.

Uncrewed Aircraft Systems (UAS) technologies offer a highly effective approach for monitoring forest health by providing the means to collect detailed data on demand. In the case of monitoring bark beetle induced disturbances, they can provide information about the spread of bark beetle infestations and support early detection of new outbreak areas to facilitate sanitary cuttings (Ecke et al., 2022). However, the suitability and commercial viability of UAS have been significantly limited by the necessity for operation primarily within visual line of sight (VLOS), making them expensive and challenging to scale across large areas. Efforts are currently ongoing to establish frameworks for beyond visual line of sight (BVLOS) UAS operation, which is expected to soon take over and enable efficient monitoring solutions for different applications. BVLOS UAS operations have been demonstrated to provide significantly more hourly endurance compared to traditional VLOS operations, with reduced fuel consumption (Slujis et al., 2023), making them suitable for large-scale monitoring operations.

Tree health assessment methods often employ machine learning methods such as Random Forest (RF) and Deep Neural Networks

(DNNs), with deep learning models generally outperforming traditional machine learning approaches (Safonova et al., 2022; Kanerva et al., 2022; Minarik et al., 2022; Junttila et al., 2022; Turkulainen et al., 2023). However, a significant challenge with deep learning models is their reliance on large amounts of labelled data. This issue is particularly pronounced in remote sensing, where changing environmental conditions can greatly increase data variability. Consequently, new reference data collection and model training are often necessary for different study areas, limiting the scalability of deep learning models. Transfer learning can mitigate this issue by utilizing models pretrained on a distinct source domain and then fine-tuning them with additional data from a new target domain (Pan & Yang, 2010), thereby reducing the need for extensive new training data. Despite its promise, the effectiveness of transfer learning for bark beetle disturbance detection, especially using source domains closely related to the target, has not been extensively investigated.

Although BVLOS operations have been successful in other fields, current scientific literature lacks studies on its application in forest health monitoring. This study presents the first results of using novel groundbreaking hydrogen-powered BVLOS airship UAS technology for monitoring forest disturbances caused by *I. typographus*. Our objective was to validate the performance of the novel technology in bark beetle damage monitoring and to explore the applicability of transfer learning techniques to enhance the scalability of deep learning models in this context.

2. Materials and Methods

2.1 Remote sensing data acquisition

Remote sensing data was collected using BVLOS operated hydrogen-powered airship technology by Kelluu Ltd. (Joensuu, Finland) (Figure 1). The airship uses hydrogen as both the lifting gas and power source, resulting in emission-free flying and data capture. The sensors for data capture are mounted on a gimbal located underneath the ship.



Figure 1. Kelluu airship on a bark beetle monitoring mission.

The study area covered 1.3 km² conserved forest area in Koli National Park, North Karelia, Finland, seriously affected by bark beetles, snow damage and drought. The UAS campaign was carried out on 13.5.2023. The flight was operated from the command centre at the Kelluu factory premises in Joensuu, approximately 75 km away from the test area, using 4G/5G communications. The mission duration was 10 hours, with transfer flights lasting 3 hours at a flight speed of 7 m/s each and the remote sensing data capture taking 4 hours at a flight speed of 5 m/s.

The Kelluu airship collected multispectral (MS) images using a Micasense RedEdge-P camera (AGEagle Aerial Systems Inc., Wichita, Kansas, USA). It comprises five bands in the blue, green, red, red-edge, and near-infrared spectral range, as well as one panchromatic band. The dataset included a total of 98928 individual images, collected with nominal forward and side overlaps of 80%. Furthermore, the airship was equipped with a Basler Ace2 RGB camera (Basler AG, Ahrensburg, Germany) that captured a total of 9309 images. The flight altitude was 105 m giving a ground sample distance (GSD) of 7 cm for the multispectral imagery and a GSD of 2 cm for the RGB imagery. Images were pre-processed into point-clouds and multispectral orthomosaics using Agisoft Metashape software (Agisoft LLC, St. Petersburg, Russia). For the MS images, the pansharpening option was not used and the radiometric calibration into reflectance values was performed using the DLS2 sensor data provided by Micasense.

2.2 Field references

In situ references were collected by forest experts. A total of 28 circular sampling plots with 10 m radius were established. 22 of the plots were damage plots established in spots of spruces showing bark beetle infestation symptoms and the remaining 6 plots were control plots with no visible symptoms of bark beetle infestation (Figure 2).

For each tree over 5 cm in diameter at breast height (dbh) within a sampling plot, tree species, dbh, height and location were recorded. Additionally, for spruce trees, trunk and crown symptoms indicating bark beetle attack were recorded and classified. The evaluated bark beetle symptoms included resin flow, entrance and exit holes, bark damage, crown discoloration and defoliation (Blomqvist et al. 2018).

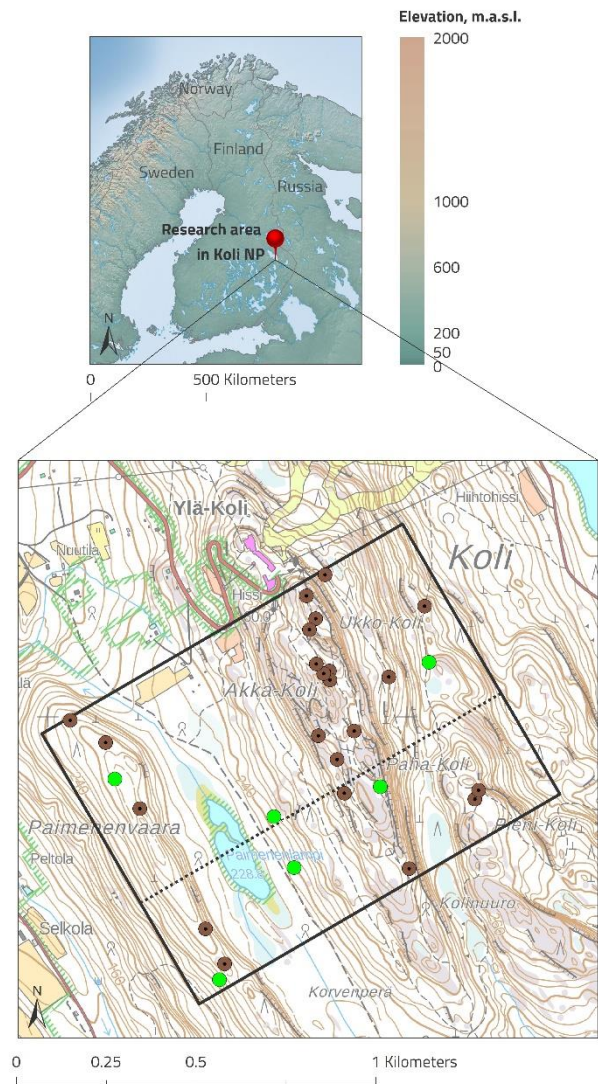


Figure 2. Field monitoring area. Brown circles show the bark beetle damage plots ($n=22$) and the green circles ($n=6$) show the control plots without bark beetle infestation. Dashed line shows the division into training and testing areas (19+9 sample plots).

The recorded trees were classified into four categories based on their species and observed discoloration symptoms. Green spruces were labelled as healthy, yellowish and reddish spruces as infested and grey spruces as dead. All other trees were classified as non-spruce.

The number of trees in each class after the labelling process is shown in Table 1. The number of recorded infested trees was very low due to the timing of the data collection. Since the data was collected in spring, crown symptoms of bark beetle infestations were not yet visible. These symptoms typically become apparent later in the season (Junttila et al., 2022).

	Healthy	Infested	Dead	Non-spruce
N-references	178	4	79	55

Table 1. Number of reference trees in each class.

2.3 Deep learning -based image analysis

2.3.1 Overview: The process includes two phases: (1) individual tree detection using the YOLOv7 network and RGB images (Wang et al., 2023), and (2) tree health analysis using MS images and a 2D-CNN classifier model as described by Turkulainen et al. (2023). The 2D-CNN model was selected for this study because it demonstrated strong performance in the investigation by Turkulainen et al. (2023), which involved multispectral images and a limited dataset. In this study, the models trained in the study by Turkulainen et al. (2023) were used as so-called base models. They were trained using datasets from the southern and southeastern Finland, 200–400 km away from the Koli test area used in this study.

Deep learning models were applied to study tree health in the disturbance area, with the special focus on examining the scalability of machine learning. Several options were studied: 1) the initial deep learning models trained in another test area, referred as base models; 2) deep learning models trained from scratch using in situ field data as reference; 3) transfer learning and fine-tuning of base models using different amounts of field reference data.

2.3.2 Data preparation: The data preparation process involved extracting individual tree crowns from the image orthomosaic and annotating datasets for object detection networks. The orthophoto captured in the research area was cropped to smaller sections, each containing a single ground sampling plot. The dimensions of the resulting images varied, with widths and heights ranging from approximately 300 to 800 pixels. Since the cropped sections were rectangular, the edges and corners often included unlabelled trees. These unlabelled trees were manually removed from the images through visual inspection. The bounding boxes for each labelled tree were manually delineated to create tree location annotations for the YOLOv7 detection network. Figure 3 shows an example of an image prepared for the YOLOv7 network. The bounding boxes are drawn on the image for visualization purposes, however, they are given to the network in text format.

To prepare the input images for the classifier networks, each reference tree crown was cropped based on its bounding box coordinates. The tree crown images were subsequently resampled into square shapes of 150×150 pixels to standardize the input dimensions. Smaller images were adjusted through padding to achieve this standard size, while larger images underwent resampling utilizing bilinear interpolation.

The reference dataset was divided into separate areas for independent training and testing sets. The study area was divided such that one half contained 19 sampling plots and the other half contained 9 sampling plots (Figure 2). The split was chosen such that each half of the research area contained an appropriate number of samples from all classes. This division ensured that the training and test sets were independent and allowed for robust evaluation of the detection and classification models.



Figure 3. Example of a prepared input image for YOLOv7.

2.3.3 Training: The base models were originally trained to only classify spruce trees into healthy, infested and dead spruce trees but in the current study a new class of non-spruce trees was introduced to enable the analysis of large forest areas with multiple tree species. In addition, in the current study the infested class was excluded due to the low or non-existent number of infested tree samples in the reference dataset.

In the transfer learning approach, the 2D-CNN model was pretrained with tree health data as described by Turkulainen et al. (2023). The model was then subjected to training with new data from the Koli region. The first layer of the network was frozen during training (Table 2). The training process consisted of 50 epochs. When training the models from scratch, all network layers were initialized randomly and trained with new data. The training was performed over 100 epochs. The hyperparameters associated with model training were optimized using the Optuna framework (Akiba et al., 2019) as described in Turkulainen et al. (2023).

2.3.4 Evaluation: The performance of the models was evaluated using various metrics, including class-wise precision, recall, and their harmonic mean, the F1-score. Additionally, overall accuracy across all classes was computed (Padilla et al., 2021; Turkulainen et al., 2023).

These metrics were calculated for the classification results obtained from the models on independent test data. Two different data splits were employed for the training and test sets. In one configuration, 19 sampling plots were used for training and validation, and 9 sampling plots were used for testing (TL fi19). In another configuration, 9 sampling plots were used for training and validation, and 19 sampling plots were used for testing (TL fi09). The data was split into training and validation sets using random sampling, with 80% of the data allocated for training and 20% for validation.

Network	Layers	Number of kernels and kernel sizes	Layer status in transfer learning	Number of trainable parameters
2D-CNN	Conv2D – BN – MaxPool –	(32) 3x3	Frozen	~200 000
	Conv2D – BN – MaxPool –	(64) 3x3	Trained	
	Conv2D – BN – AvgPool –	(64) 3x3	Trained	
	FC – Dropout – FC		Trained	

Table 2. 2D-CNN architecture and transfer learning configuration. FC: Fully connected layer; BN: Batch normalization.

3. Results and discussion

The results of the different training options are shown in Table 3 and Figure 4. The base model exhibited the poorest overall performance, with F1-scores of 0.726 and 0.894 for healthy and dead trees, respectively. In contrast, the model trained from scratch using only data from the new study area achieved significantly better overall performance, with F1-scores of 0.914, 0.857 and 0.647 for healthy, dead and non-spruce trees.

When training the 2D-CNN model using transfer learning and fine-tuning techniques and the larger training dataset, the F1-scores improved significantly across all categories. The model achieved F1-scores of 0.936, 0.955, and 0.817 for healthy, dead, and non-spruce trees, respectively. Using a smaller training

dataset, the model achieved F1-scores 0.942, 0.891 and 0.581 for healthy, dead and non-spruce trees.

These results indicated that the best approach for tree health classification with the 2D-CNN network was to use transfer learning and fine-tuning of the pretrained base model with a larger field reference dataset for training. Without transfer learning, the F1-scores on the same dataset were 2% poorer for healthy spruces, 10% poorer for dead spruces, and 21% poorer for non-spruce trees. In comparison, using transfer learning with a smaller field reference dataset showed no significant change for healthy trees but resulted in decreases of 7% and 29% of F1-scores for dead and non-spruce trees, respectively. Direct testing of the base model on new data without additional fine-tuning and training resulted in a 22% decrease in F1-scores for healthy trees and a 6% decrease for dead trees compared to the transfer learning approach using the larger dataset.

Model	OA	Class	Precision	Recall	F1-score	N-reference Tr; Va; Te
base model	0.665	Healthy	0.803	0.663	0.726	558; 129; 178
		Dead	0.835	0.962	0.894	374; 93; 79
noTL fi19	0.824	Healthy	0.885	0.945	0.914	84; 21; 73
		Dead	0.750	1.00	0.857	46; 12; 21
		Non-spruce	0.846	0.524	0.647	10; 3; 42
TL fi19	0.904	Healthy	0.880	1.00	0.936	84; 21; 73
		Dead	0.913	1.00	0.955	46; 12; 21
		Non-spruce	1.00	0.690	0.817	10; 3; 42
TL fi09	0.883	Healthy	0.960	0.924	0.942	58; 15; 105
		Dead	0.869	0.914	0.891	17; 4; 58
		Non-spruce	0.500	0.692	0.581	34; 8; 13

Table 3. Classification results of 2DCNN network. Numbers of reference trees in the training (Tr), validation (Va), and test (Te) sets are also given. TL: Transfer learning; noTL: No transfer learning used; fi: Field inventory.

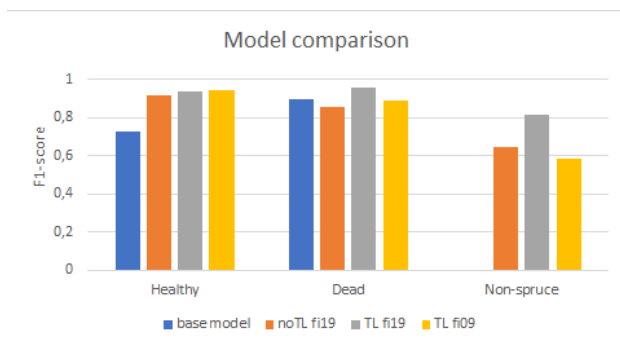


Figure 4. Visualisation of the classification results for each model.

The classification accuracy for the non-spruce class was consistently lower than for the healthy and dead classes. This disparity was especially pronounced in the approaches that did not employ transfer learning. While the accuracies for healthy and dead spruce trees were high with approximately 50 to 60 training samples, the accuracy for the non-spruce class was typically low with the same number of samples. This discrepancy can likely be attributed to the high variability within the training samples for non-spruce trees. The non-spruce class included both Scots pines (*Pinus sylvestris* L.) and deciduous trees, which displayed distinct characteristics in the images. Pines visually resembled healthy spruce trees, whereas deciduous trees appeared similar to dead trees, as they were leafless during springtime. The confusion matrix for the results of the TL fi19 model (Table 4) demonstrates that, while all healthy and dead spruces were correctly classified, the model misclassified many

non-spruce samples as healthy spruces and some as dead spruce trees. This suggests that robust classification of the non-spruce class necessitates more training data.

		Measured		
		Healthy	Dead	Non-spruce
Predicted	Healthy	73	0	10
	Dead	0	21	2
	Non-spruce	0	0	29

Table 4. Confusion matrix for the model trained using transfer learning and large field reference dataset (TL fi19).

A comparison between the large (19 training plots) and small (9 training plots) training datasets revealed that the classification results for the more easily identifiable healthy and dead classes were quite similar. However, the smaller training dataset yielded significantly poorer results for the non-spruce class. Interestingly, the larger training dataset included fewer training samples for non-spruce classes than the smaller training dataset due to the way the datasets were divided in the field. This further suggests that the number of non-spruce samples was insufficient, preventing the robust and accurate classification of this class.

The results were comparable to a previous study by Turkulainen et al. (2023), where the 2D-CNN model produced F-scores of 0.911, 0.722 and 0.895 for healthy, infested and dead classes respectively, using MS-data captured by drones from study areas in southern and southeast Finland. These results indicate that Kelluu BVLOS airships offered accuracy comparable to classical VLOS UAS technology. Compared to satellites or manned aircraft, cloud cover posed less interference, as flights were conducted below the clouds. This underscores the effectiveness of the approach in reliably capturing remote sensing images and supporting applications requiring rapid responses.

The TL fi19 model was employed to detect and classify the health of all trees in the study area. The damage map generated for the entire research area provided insight into bark beetle damage in Koli National Park (Figure 5). Bark beetle damage was most prominent at high elevations and mature conifer-dominated areas. At the western slope of Koli Hill, where the stands are middle-aged and dominated by deciduous species mixed with coniferous species, the damage was less prominent despite high elevation.

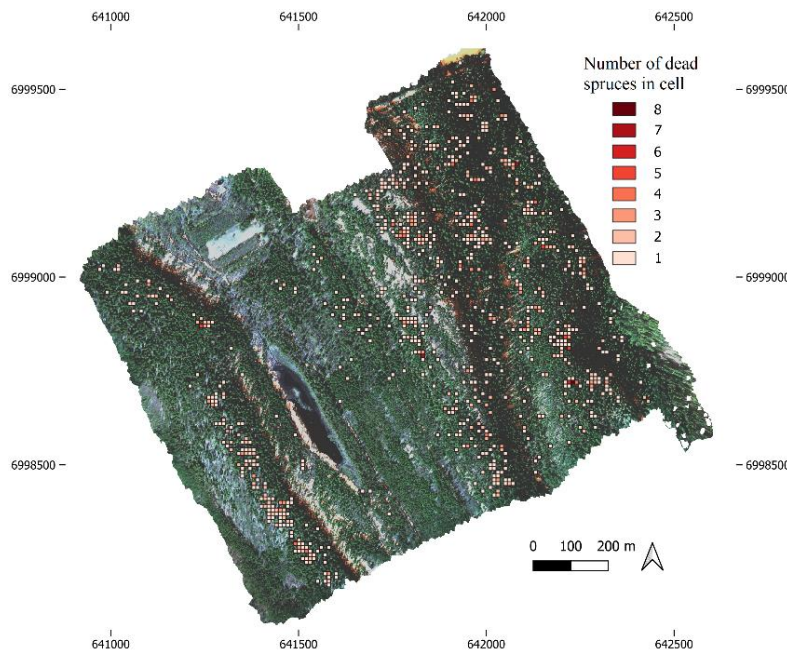


Figure 5. Number of identified dead spruces in each 10 m by 10 m cell.

The results emphasize the advantages of utilizing transfer learning in remote sensing applications. Specifically, in the context of tree health analysis, classification accuracy improves when a model pretrained with tree health data is employed, supplemented with a small number of new training samples. This approach outperforms both using a pretrained model to analyse a new area without additional training and training a model entirely from scratch without leveraging a pretrained model.

4. Conclusions

This research demonstrates the potential of innovative BVLOS UAS operations for large-scale forest health monitoring. The study specifically targeted detection and classification of tree disturbances caused by *I. typographus*. Our findings indicate that BVLOS UAS technology, such as that developed by Kelluu Ltd.,

can effectively overcome the operational limitations of traditional VLOS systems, providing a scalable solution for extensive forest monitoring tasks.

The application of advanced deep learning techniques, particularly transfer learning, significantly enhanced the accuracy of tree health classification. Models fine-tuned with extensive field reference data achieved high F1-scores of 0.936 for healthy trees, 0.955 for dead trees, and 0.817 for non-spruce classes, outperforming models trained from scratch. These results affirm the advantages of transfer learning in improving model performance with less training data, thus addressing one of the major challenges in remote sensing applications.

Despite the overall success, the classification accuracy for the non-spruce class remained quite low compared to healthy and

dead classes, especially without the benefit of transfer learning. This highlights the need for more diverse and comprehensive training datasets to capture the variability within non-spruce tree samples in future studies.

Overall, this study validates the use of hydrogen-powered BVLOS airships as a pioneering approach to forest health monitoring. The integration of advanced UAS technology with deep learning and transfer learning methodologies provides a robust framework for the accurate and scalable detection of forest disturbances. Future research should focus on improving data collection methods for non-spruce trees, further refining transfer learning techniques, and expanding studies to include the classification of infested trees, which was limited in this study due to insufficient reference data caused by the conditions in the target area.

Acknowledgements

We wish to thank Heini Kanerva, Diana-Cristina Simon and Ari Voutilainen for the help with the fieldwork. We also greatly appreciate the assistance of Erika Vennervirta in conducting image-based annotations. Metsähallitus is thanked for enabling this study in Koli National Park.

This work was supported by the European Commission under Grant 101078970; the Research Council of Finland under Grants 353263, 353264, 357380; the Ministry of Agriculture and Forestry of Finland under Grants VN/5292/2021, VN/3482/2021. This project received funding from the European Union – NextGenerationEU instrument. This study was affiliated to the Research Council of Finland Flagship Forest–Human–Machine Interplay—Building Resilience, Redefining Value Networks and Enabling Meaningful Experiences (UNITE) (Grant 357908).

5. References

Akiba, T., Sano, S., Yanase, T., Ohta, T., & Koyama, M. 2019. Optuna: A Next-generation Hyperparameter Optimization Framework. *Proceedings of the 25th ACM SIGKDD International Conference on Knowledge Discovery & Data Mining*, 2623–2631. <https://doi.org/10.1145/3292500.3330701>

Barrere, J., Reineking, B., Cordonnier, T., Kulha, N., Honkaniemi, J., Peltoniemi, M., Korhonen, K. T., Ruiz-Benito, P., Zavala, M. A., & Kunstler, G. 2023. Functional traits and climate drive interspecific differences in disturbance-induced tree mortality. *Global Change Biology*, 29(10), 2836–2851. <https://doi.org/10.1111/gcb.16630>

Blomqvist, M., Kosunen, M., Starr, M., Kantola, T., Holopainen, M., & Lyytikäinen-Saarenmaa, P. 2018. Modelling the predisposition of Norway spruce to *Ips typographus* L. infestation by means of environmental factors in southern Finland. *European Journal of Forest Research*, 137(5), 675–691. <https://doi.org/10.1007/s10342-018-1133-0>

Ecke, S., Dempewolf, J., Frey, J., Schwaller, A., Endres, E., Klemmt, H.-J., Tiede, D., & Seifert, T. 2022. UAV-Based Forest Health Monitoring: A Systematic Review. *Remote Sensing*, 14(13), 3205. <https://doi.org/10.3390/rs14133205>

Junttila, S., Näsi, R., Koivumäki, N., Imangholiloo, M., Saarinen, N., Raisio, J., Holopainen, M., Hyyppä, H., Hyyppä, J., Lyytikäinen-Saarenmaa, P., Vastaranta, M., & Honkavaara, E. 2022. Multispectral Imagery Provides Benefits for Mapping

Spruce Tree Decline Due to Bark Beetle Infestation When Acquired Late in the Season. *Remote Sensing*, 14(4), 909. <https://doi.org/10.3390/rs14040909>

Kanerva, H., Honkavaara, E., Näsi, R., Hakala, T., Junttila, S., Karila, K., Koivumäki, N., Alves Oliveira, R., Pelto-Arvo, M., Pölönen, I., Tuviala, J., Östersund, M., & Lyytikäinen-Saarenmaa, P. 2022. Estimating Tree Health Decline Caused by *Ips typographus* L. from UAS RGB Images Using a Deep One-Stage Object Detection Neural Network. *Remote Sensing*, 14(24), 6257. <https://doi.org/10.3390/rs14246257>

Mensink, T., Uijlings, J., Kuznetsova, A., Gygli, M., & Ferrari, V. 2022. Factors of Influence for Transfer Learning Across Diverse Appearance Domains and Task Types. *IEEE Transactions on Pattern Analysis and Machine Intelligence*, 44(12), 9298–9314. <https://doi.org/10.1109/TPAMI.2021.3129870>

Minařík, R., Langhammer, J., & Lendzioch, T. 2021. Detection of Bark Beetle Disturbance at Tree Level Using UAS Multispectral Imagery and Deep Learning. *Remote Sensing*, 13(23), 4768. <https://doi.org/10.3390/rs13234768>

Padilla, R., Passos, W. L., Dias, T. L. B., Netto, S. L., & Da Silva, E. A. B. 2021. A Comparative Analysis of Object Detection Metrics with a Companion Open-Source Toolkit. *Electronics*, 10(3), 279. <https://doi.org/10.3390/electronics10030279>

Pan, S. J., & Yang, Q. 2010. A Survey on Transfer Learning. *IEEE Transactions on Knowledge and Data Engineering*, 22(10), 1345–1359. <https://doi.org/10.1109/TKDE.2009.191>

Patacca, M., Lindner, M., Lucas-Borja, M. E., Cordonnier, T., Fidej, G., Gardiner, B., Hauf, Y., Jasinevičius, G., Labonne, S., Linkevicius, E., Mahnken, M., Milanovic, S., Nabuurs, G., Nagel, T. A., Nikinmaa, L., Panyatov, M., Bercak, R., Seidl, R., Ostrogović Sever, M. Z., ... Schelhaas, M. 2023. Significant increase in natural disturbance impacts on European forests since 1950. *Global Change Biology*, 29(5), 1359–1376. <https://doi.org/10.1111/gcb.16531>

Safonova, A., Hamad, Y., Alekhina, A., & Kaplun, D. 2022. Detection of Norway Spruce Trees (*Picea Abies*) Infested by Bark Beetle in UAV Images Using YOLOs Architectures. *IEEE Access*, 10, 10384–10392. <https://doi.org/10.1109/ACCESS.2022.3144433>

Turkulainen, E., Honkavaara, E., Näsi, R., Oliveira, R. A., Hakala, T., Junttila, S., Karila, K., Koivumäki, N., Pelto-Arvo, M., Tuviala, J., Östersund, M., Pölönen, I., & Lyytikäinen-Saarenmaa, P. 2023. Comparison of Deep Neural Networks in the Classification of Bark Beetle-Induced Spruce Damage Using UAS Images. *Remote Sensing*, 15(20), 4928. <https://doi.org/10.3390/rs15204928>

Van Der Sluijs, J., Saiet, E., Bakelaar, C. N., Wentworth, A., Fraser, R. H., & Kokelj, S. V. 2023. Beyond visual-line-of-sight (BVLOS) drone operations for environmental and infrastructure monitoring: A case study in northwestern Canada. *Drone Systems and Applications*, 11, 1–15. <https://doi.org/10.1139/dsa-2023-0012>

Wang, C.-Y., Bochkovskiy, A., & Liao, H.-Y. M. 2022. *YOLOv7: Trainable bag-of-freebies sets new state-of-the-art for real-time object detectors* (arXiv:2207.02696). arXiv. <https://arxiv.org/abs/2207.02696>